DIFFERENTIATE-AND-FIRE TIME-ENCODING OF FINITE-RATE-OF-INNOVATION SIGNALS

Abijith Jagannath Kamath 🆔 *and Chandra Sekhar Seelamantula* 🆔

Department of Electrical Engineering, Indian Institute of Science, Bangalore 560012.
Email:{abijithj, css}@iisc.ac.in

ABSTRACT

Time-encoding or *event-driven sampling* of continuous-time signals is an alternative paradigm to uniform sampling. In this sampling scheme, the signal is encoded by a sequence of time-instants as opposed to a sequence of amplitudes in uniform sampling. Time-encoding is opportunistic by design – measurements are taken only when the signal exhibits significant variability. Consequently, the measurements are sparse, noise-robust, and require low power. However, standard processing and reconstruction methods do not apply. In this paper, we introduce a new time-encoding machine, namely, differentiate-and-fire time-encoding machine (DIF-TEM) inspired by the functioning of the human visual system. A DIF-TEM can be tuned to provide sampling sets with variable densities – sparse sets that mimic dynamic vision sensors (neuromorphic cameras) or dense sets that mimic classical time-encoding machines. We propose kernel-based time-encoding of finite-rate-of-innovation (FRI) signals using DIF-TEM via Fourier-domain analysis. We show that DIF-TEM measurements are sufficient for perfect signal reconstruction under certain conditions. We provide simulation results to substantiate our claims.

Index Terms— Time-encoding machine, event-driven sampling, neuromorphic camera, finite-rate-of-innovation, differentiate-and-fire time-encoding machine.

1. INTRODUCTION

In Shannon's sampling [1], uniform samples of a signal or its filtered version constitute an accurate discrete representation with perfect reconstruction guarantees. Shannon's sampling theorem [2] forms the foundation of analog-to-digital conversion of continuous-time bandlimited signals. Uniform sampling is used in modern digital cameras such as CMOS or APS-C based cameras. Recently, a new class of sampling devices called time-encoding machines (TEM) have been proposed, which are inspired by neural encoding of sensory stimuli [3, 4]. TEMs encode signals by a sequence of time-instants that are nonuniformly spaced and correspond to the occurrence of an event. Effectively, time-encoding machines are *event-driven sampling schemes*. Lazar [5] introduced the *integrate-and-fire time-encoding machine* (IF-TEM) that records nonuniform *trigger times*, which contain information about local signal averages. Gontier and Vetterli [6] showed that the IF-TEM is closely linked to generalized zero-crossing/level-crossing encoding and developed the crossing-time-encoding machine (C-TEM). They showed the IF-TEM, is in fact, the adjoint of the C-TEM — and therefore, similar
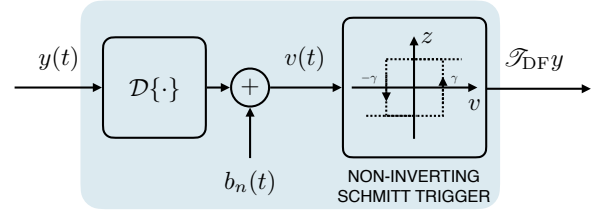
Fig. 1. A differentiate-and-fire time-encoding machine (DIF-TEM) with a bias signal $b_n(t)$. The sum of the differentiated signal $\mathcal{D}y(t)$ and the bias is fed into a non-inverting Schmitt trigger. The transition times of the bilevel signal $z(t; \mathscr{T}_{\mathrm{DF}}y)$ is provided as the output of the DIF-TEM.

strategies using the method of alternating projections onto convex sets (PoCS) [7] can be used for signal reconstruction from C-TEM or IF-TEM measurements.

Recent developments in neuromorphic computing have introduced neuro-inspired visual sensors called Dynamic Vision Sensors (DVS) [8, 9]. The DVS represents scenes asynchronously at each pixel in the *address event representation* (AER) that encodes the time-instant and the polarity at which the incident light intensity, more precisely, the log-intensity, changes by a preset threshold, which defines an event. A scene is represented as sequence of events rather than a sequence of uniformly occurring frames. The interpretation is not trivial as in the case of conventional frame based cameras. The data does not offer a ready visualization of the scene and additional processing becomes necessary to reconstruct the scene from the measurements. On the upside, the acquisition is asynchronous, uses low power, and has high temporal resolutions, of the order of a microsecond. Scene reconstruction from neuromorphic events can be performed using integration based methods [10, 11].

1.1. Contribution of this Paper

In this paper, we consider the *differentiate-and-fire time-encoding machine* (DIF-TEM) as opposed to the integrate-and-fire TEM. A schematic of DIF-TEM is shown in Fig. 1. The DIF-TEM is inspired by the magnocellular pathways in human vision system [12], which specialize in detecting high-rate transient events as opposed to the IF-TEM, which we believe is a perfect fit for the parvocellular pathways that detect slow and sustained stimuli. Neuromorphic cameras are also inspired by the magnocellular pathways and record sparse events. The DIF-TEM is a novel sampling strategy modeled after the operation of a neuromorphic camera. A DIF-TEM (Sec. 2) encodes signals using nonuniform trigger times together with the corresponding samples of the derivative of the signal. We first introduced DIF-TEM recently in [13], wherein we showed that bandlimited signals

and signals lying in shift-invariant spaces can be reconstructed from DIF-TEM measurements using the method of alternating projections onto convex sets [7]. In this paper, we consider DIF-TEM sampling of signals with a finite rate of innovation (FRI) [14] (Sec. 3). We provide sufficient conditions for perfect reconstruction and present simulation results to support the claims (Sec. 4).

There is abundant literature on derivative based sampling and it is not feasible to review them all in a conference paper. We refer the reader to the books by Marvasti [15] and Marks [16]. To the best of our knowledge, this paper is the first one to propose the DIF-TEM sampling scheme for FRI signals.

2. DIFFERENTIATE-AND-FIRE TIME-ENCODING MACHINE

Gontier and Vetterli [6] abstracted a TEM as a map from the space of real-valued functions $\mathbb{R}^{\mathbb{R}}$ to the space of real-valued sequences $\mathbb{R}^{\mathbb{Z}}$ with increasing entries, and provided the following definition.

Definition 1. *A time-encoding machine with an event operator* $\mathscr{E}$: $\mathbb{R}^{\mathbb{R}} \to \mathbb{R}^{\mathbb{R}}$ *and references* $\{r_n \in \mathbb{R}^{\mathbb{R}}\}_{n \in \mathbb{Z}}$ *is a map* $\mathscr{T} : \mathbb{R}^{\mathbb{R}} \to \mathbb{R}^{\mathbb{Z}}$ *such that* $\mathbb{R}^{\mathbb{R}} \ni y \mapsto \mathscr{T}y$, *with*

 a. $\mathscr{T}y = \{t_i \in \mathbb{R} \mid t_i > t_j, \ \forall i > j, i \in \mathbb{Z}\}$,
 b. $\lim_{n \to \pm\infty} t_n = \pm\infty$, *and*
 c. $(\mathscr{E}y)(t_n) = r_n(t_n), \forall t_n \in \mathscr{T}y$.

The above definition is an alternative to considering a C-TEM as a nonuniform sampling device and the IF-TEM as its adjoint. The identity event operator and a sinusoidal reference gives the C-TEM. On the other hand, an accumulator event operator and a constant reference gives the IF-TEM [17]. The above definition allows one to consider a generalized event operator $\mathscr{E}$ and references $\{r_n\}_{n \in \mathbb{Z}}$.

Consider the DIF-TEM shown in Fig. 1 with parameters $\{\alpha, \gamma\}$, and a linear bias $b_n(t) = (-1)^n \alpha (t - t_{n-1})_+$, where t_{n-1} belongs to the output $\mathscr{T}_{\mathrm{DF}}y$. The notation $(t)_+$ denotes $\max\{t, 0\}$. The input signal $y(t)$ is differentiated and added to the linear bias to get $v(t)$, which is then fed to a non-inverting Schmitt trigger with threshold γ. Suppose, in the positive cycle, $v(t)$ exceeds γ at $t = t_n$, then the linear term resets to intercept the time axis at t_n which is also included in the output $\mathscr{T}_{\mathrm{DF}}y$ and the sign of α flips. Similarly, an output is generated in the negative cycle if $v(t)$ subceeds $-\gamma$. The output of the Schmitt trigger is a bi-level signal $z(t; \mathscr{T}_{\mathrm{DF}}y)$ with transitions at the locations in the entries of $\mathscr{T}_{\mathrm{DF}}y$. The transition times can be obtained from the bi-level signal using sub-Nyquist methods in [14,18]. The output of the DIF-TEM $\mathscr{T}_{\mathrm{DF}}y$ has increasing entries that satisfy the following lemma.

Lemma 1. *(t-transform) Let* $y \in \mathcal{C}^1(\mathbb{R})$ *be the input to the DIF-TEM with parameters* $\{\alpha, \gamma\}$. *The output of the DIF-TEM* $\mathscr{T}_{\mathrm{DF}}y = \{t_n\}_{n \in \mathbb{Z}}$ *satisfies:*

$$(\mathcal{D}y)(t_n) = (-1)^{n+1} (\gamma - \alpha(t_n - t_{n-1})), \ \forall t_n \in \mathscr{T}_{\mathrm{DF}}y. \quad (1)$$

Proof. Without loss of generality, consider the Schmitt trigger to be in the positive cycle after $t = t_0$. The next trigger time $t = t_1$ satisfies

$$\mathcal{D}y(t) + \alpha(t - t_0)\big|_{t=t_1} = \gamma. \quad (2)$$

The second trigger time obtained in the negative cycle at $t = t_2$ satisfies

$$\mathcal{D}y(t) - \alpha(t - t_1)\big|_{t=t_2} = -\gamma. \quad (3)$$

Combining Eqs. (2) and (3) and generalizing for subsequent trigger times results in Eq. (1). □

Lemma 1 is the counterpart of the "t-transform" that computes local averages of the input from the output of the IF-TEM [5]. Lemma 1 ensures that the DIF-TEM satisfies Definition 1 with the differentiation event operator and linear references defined as $r_n(t) = (-1)^{n+1} (\gamma - \alpha(t - t_{n-1}))$, $t \in [t_n, t_{n-1}[$. The DIF-TEM output contains information about the samples of the derivative of the input. The operation of the DIF-TEM in the particular case where $\alpha = 0$ mimics the DVS. The introduction of the bias enables direct control over the frequency of the events, and thus the sampling density of $\mathscr{T}_{\mathrm{DF}}y$.

Corollary 1. *(Sampling sets of DIF-TEM) Let* $y \in \mathcal{C}^1(\mathbb{R})$ *with* $\|\mathcal{D}y\|_\infty \leq \beta$ *be the input to the DIF-TEM with parameters* $\{\alpha, \gamma\}$ *(cf. Fig. 1). The output of the DIF-TEM* $\mathscr{T}_{\mathrm{DF}}y = \{t_n\}_{n \in \mathbb{Z}}$ *satisfies*

$$\frac{\gamma - \beta}{\alpha} \leq t_n - t_{n-1} \leq \frac{\gamma + \beta}{\alpha}. \quad (4)$$

Corollary 1 ensures that the sampling set is $\dfrac{\gamma - \beta}{\alpha}$-distinct when $\gamma \geq \beta$ and the sampling density $d(\mathscr{T}_{\mathrm{DF}}y) \doteq \sup_{n \in \mathbb{Z}} |t_n - t_{n-1}|$ of the DIF-TEM is bounded above by $\dfrac{\gamma + \beta}{\alpha}$, whenever $\alpha > 0$, for all inputs that have a bounded derivative. With $\alpha = 0$, the sampling density is unbounded for any input, which is the case with the neuromorphic camera where the encoding is sparse. With low α, the sampling set is sparse, and with high α, the sampling set is dense.

3. TIME-ENCODING OF FRI SIGNALS USING DIF-TEM

In this section, we consider time-encoding of FRI signals [14] using a DIF-TEM. Consider the T-periodic FRI signal $x \in L^2([0, T[)$ consisting of a linear combination of K time-shifted pulses:

$$x(t) = \sum_{m \in \mathbb{Z}} \sum_{k=0}^{K-1} c_k \varphi(t - \tau_k - mT), \quad (5)$$

where $\varphi \in L^2(\mathbb{R})$ is a known pulse and $\mathbf{c} = [c_0 \ c_1 \ \cdots \ c_{K-1}]^{\mathsf{T}} \in \mathbb{R}^K$ and $\boldsymbol{\tau} = [\tau_0 \ \tau_1 \ \cdots \ \tau_{K-1}]^{\mathsf{T}} \in \mathbb{R}^K$ are unknown amplitudes and shifts, respectively, that completely specify the signal. This is the canonical FRI signal model that extends to aperiodic FRI signals, piecewise polynomials, and signals in shift-invariant spaces including bandlimited signals. Clearly, the signal has a rate of innovation of $\dfrac{2K}{T}$, which is also the minimum sampling requirement [19]. We consider kernel-based time-encoding, i.e., the FRI signal is passed through a sampling kernel $g(t)$ prior to time-encoding (cf. Fig. 2). The reconstruction problem at hand is to determine $x(t)$, or equivalently, the parameters $\mathbf{c}$ and $\boldsymbol{\tau}$, from time-encoded measurements $\mathscr{T}_{\mathrm{DF}}y$, where $y(t) = (x * g)(t)$. The FRI signal $x(t)$ in Eq. (5) is the dual of a linear combination of complex sinusoids, which is a familiar model in parametric spectral estimation [20]. Since $x(t) \in L^2([0, T[)$, its Fourier coefficients, using Poisson summation formula, are given by

$$\hat{x}_m = \frac{1}{T} \hat{\varphi}(m\omega_0) \sum_{k=0}^{K-1} c_k e^{-\mathrm{j}\omega_0 m \tau_k}, \ m \in \mathbb{Z}, \quad (6)$$

where $\omega_0 = \dfrac{2\pi}{T}$ and $\hat{\varphi}$ denotes the Fourier transform of the pulse φ. Estimation of the shifts $\{\tau_k\}_{k=0}^{K-1}$ is possible using Prony's method [14, 21] using the $N = 2M + 1$ contiguous coefficients in $\hat{\mathbf{x}} =$

$\left[\dfrac{\hat{x}_{-M}}{\hat{\varphi}(-M\omega_0)} \cdots \dfrac{\hat{x}_M}{\hat{\varphi}(M\omega_0)}\right]^{\mathsf{T}} \in \mathbb{C}^N$, where $K \leq M \in \mathbb{N}$. We assume that the pulse φ has finite duration such that $\hat{\varphi}(m\omega_0)$ does not vanish for $m \in [\![-M, M]\!]$. Once the shift parameters are estimated, the amplitudes $\mathbf{c}$ can be estimated by solving the linear system of equations $\hat{\mathbf{x}} = \mathbf{V}(\boldsymbol{\tau})\mathbf{c}$, where $\mathbf{V}(\boldsymbol{\tau}) \in \mathbb{C}^{N \times K}$ has entries defined by $[\mathbf{V}(\boldsymbol{\tau})]_{i,j} = \dfrac{1}{T}e^{-\mathrm{j}\omega_0(i-M-1)\tau_{j-1}}$. The matrix $\mathbf{V}(\boldsymbol{\tau})$ is left-invertible when $N \geq K$ and the shift parameters are distinct since it has a Vandermonde structure [22].

3.1. Kernel-based Time-Encoding

Consider kernel-based time-encoding (Fig. 2). Filtering the FRI signal $x(t)$ in Eq. (5) using a sampling kernel $g(t) \in L^2(\mathbb{R})$ yields

$$
\begin{aligned}
y(t) = (x * g)(t) &= \int_{\mathbb{R}} g(\nu)x(t-\nu)\,\mathrm{d}\nu, \\
&= \int_{\mathbb{R}} g(\nu) \sum_{m \in \mathbb{Z}} \hat{x}_m e^{\mathrm{j}\omega_0 m(t-\nu)}\,\mathrm{d}\nu, \\
&= \sum_{m \in \mathbb{Z}} \hat{x}_m \left(\int_{\mathbb{R}} g(\nu)e^{-\mathrm{j}\omega_0 m\nu}\,\mathrm{d}\nu\right) e^{\mathrm{j}\omega_0 mt}, \\
&= \sum_{m \in \mathbb{Z}} \hat{x}_m \hat{g}(m\omega_0)e^{\mathrm{j}\omega_0 mt},
\end{aligned}
\tag{7}
$$

where $\hat{g}$ denotes the Fourier transform of g. The filtered signal $y(t)$ is also T-periodic with Fourier coefficients $\{\hat{x}_m \hat{g}(m\omega_0)\}_{m \in \mathbb{Z}}$. Assume that the sampling kernel satisfies Fourier-domain alias-cancellation conditions [23]:

$$
\hat{g}(\omega) = \begin{cases} g_m \neq 0, & \omega = m\omega_0, m \in [\![-M, M]\!], \\ 0, & \omega = m\omega_0, m \notin [\![-M, M]\!], \\ \text{arbitrary}, & \text{otherwise}. \end{cases}
\tag{8}
$$

Examples of such kernels include the sinc function of bandwidth $\dfrac{2M+1}{T}$, where $g_m = 1, \forall m \in [\![-M, M]\!]$; the sum-of-sincs (SoS) kernel in the Fourier domain [24]; the sum-of-modulated-spline (SMS) kernels in the time domain [23]; and exponential-reproducing and polynomial-reproducing kernels, which satisfy the generalised Strang-Fix conditions [25]. Setting $g_m = 1, \forall m \in [\![-M, M]\!]$ in Eq. (8), without loss of generality, we have

$$
y(t) = (x * g)(t) = \sum_{m=-M}^{M} \hat{x}_m e^{\mathrm{j}\omega_0 mt}.
\tag{9}
$$

Let $\mathscr{T}_{\mathrm{DF}}y = \{t_n\}_{n \in \mathbb{Z}}$ be the output of the DIF-TEM with parameters $\{\alpha, \gamma\}$ and the filtered signal $y(t) = (x * g)(t)$ as the input. The samples of the derivative can be computed from the output of the DIF-TEM, using Lemma 1, and they take the form:

$$
y_n \doteq (\mathcal{D}y)(t_n) = \sum_{m=-M}^{M} \hat{x}_m \cdot (\mathrm{j}\omega_0 m) \cdot e^{\mathrm{j}\omega_0 mt_n}.
\tag{10}
$$

Consider L measurements in the interval $[0, T[$. We obtain a linear system of equations of the form $\mathbf{y} = \mathbf{G}_{\mathrm{DF}}\mathbf{S}\hat{\mathbf{x}}$, where $\hat{\mathbf{x}} = [\hat{x}_{-M} \cdots \hat{x}_0 \cdots \hat{x}_M]^{\mathsf{T}} \in \mathbb{C}^N$ is the vector of Fourier coefficients, $\mathbf{y} = [y_1\ y_2\ \cdots\ y_L]^{\mathsf{T}} \in \mathbb{R}^L$ is the vector of samples of the derivative, $\mathbf{S} = \mathrm{diag}\left(\{\mathrm{j}\omega_0 m\}_{m=-M}^{M}\right) \in \mathbb{C}^{N \times N}$ is a diagonal
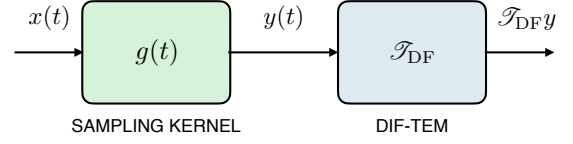

Fig. 2. Kernel-based time-encoding of $x(t)$ using a sampling kernel $g(t)$ and DIF-TEM $\mathscr{T}_{\mathrm{DF}}$.

matrix, and $\mathbf{G}_{\mathrm{DF}} \in \mathbb{C}^{L \times N}$ is the forward transformation given by:

$$
\mathbf{G}_{\mathrm{DF}} = \begin{bmatrix} e^{-\mathrm{j}M\omega_0 t_1} & \cdots & e^{-\mathrm{j}\omega_0 t_1} & 1 & e^{\mathrm{j}\omega_0 t_1} & \cdots & e^{\mathrm{j}M\omega_0 t_1} \\ e^{-\mathrm{j}M\omega_0 t_2} & \cdots & e^{-\mathrm{j}\omega_0 t_2} & 1 & e^{\mathrm{j}\omega_0 t_2} & \cdots & e^{\mathrm{j}M\omega_0 t_2} \\ \vdots & & \vdots & \vdots & \vdots & & \vdots \\ e^{-\mathrm{j}M\omega_0 t_L} & \cdots & e^{-\mathrm{j}\omega_0 t_L} & 1 & e^{\mathrm{j}\omega_0 t_L} & \cdots & e^{\mathrm{j}M\omega_0 t_L} \end{bmatrix}.
\tag{11}
$$

Lemma 2. *The matrix $\mathbf{G}_{\mathrm{DF}}$ defined in Eq. (11) has full column-rank when $L \geq N$.*

The proof is similar to [17, Lemma 3] where we use the properties of Vandermonde matrices and the fact the the sampling set is $\dfrac{\gamma - \beta}{\alpha}$-distinct and hence has full column-rank whenever $L \geq N$. The diagonal matrix $\mathbf{S}$ is not invertible since the entries on the diagonal are not all nonzero. In particular, the entry corresponding to the scaling of the zeroth Fourier coefficient is zero. Hence, the zeroth Fourier coefficient cannot be uniquely retrieved, i.e., the signal can only be recovered up to a global constant offset.

The Fourier coefficients $\{\hat{x}_m | m \in [\![-M, M]\!] \setminus \{0\}\}$ can be uniquely recovered by resetting $\mathbf{S}_{M+1, M+1} = 1$ and solving the linear system of equations $\mathbf{y} = \mathbf{G}_{\mathrm{DF}}\mathbf{S}\hat{\mathbf{x}}$. Setting $\hat{x}_0 = 0$, the shift parameters are obtained using Prony's method and then the amplitude parameters are obtained by solving the linear system of equations $\hat{\mathbf{x}} = \mathbf{V}(\boldsymbol{\tau})\mathbf{c}$.

3.2. Sufficient Conditions for Perfect Recovery

Let the filtered signal $y(t) = (x * g)(t)$ be observed using a DIF-TEM with parameters $\{\alpha, \gamma\}$ (cf. Fig. 1). Further, let $y(t)$ have bounded derivative, i.e., $\|\mathcal{D}y\|_\infty \leq \beta$. Using Corollary 1, the sampling density of the output $\mathscr{T}_{\mathrm{DF}}y$ is bounded by $\dfrac{\gamma + \beta}{\alpha}$. To obtain $L \geq 2M + 1 \geq 2K + 1$ time-instants in the interval $[0, T[$, the parameters of the DIF-TEM must satsify:

$$
L\frac{\gamma + \beta}{\alpha} \leq T.
$$

We summarize the preceding discussion in the following proposition.

Proposition 1. *(Sufficient condition for perfect recovery of FRI signals from DIF-TEM measurements) Let the T-periodic FRI signal $x(t)$ in Eq. (5) be observed using a sampling kernel $g(t)$ that satisfies Eq. (8) and a DIF-TEM with parameters $\alpha, \gamma > 0$. The time instants $\{t_n\}_{n=1}^{L} \subset \mathscr{T}_{\mathrm{DF}} \cap [0, T[$ constitute a sufficient representation of x if $L \geq 2K + 1$ and the parameters of the DIF-TEM satisfy*

$$
\frac{\gamma + \|x * \mathcal{D}g\|_\infty}{\alpha} \leq \frac{T}{L}.
\tag{12}
$$

4. SIMULATION RESULTS

Consider the periodic FRI signal

$$x_1(t) = \sum_{m \in \mathbb{Z}} \sum_{k=0}^{4} c_k \varphi(t - \tau_k - m), \qquad (13)$$

where the pulse $\varphi(t) = \beta^{(3)}(10t)$, $\beta^{(3)}$ being the centered cubic B-spline [26]. In Eq. (13), the amplitudes are set to $\{c_k\}_{k=0}^{4} = \{0.49, -0.65, 0.46, -0.52, 0.21\}$ and the shifts are set to $\{\tau_k\}_{k=0}^{4} = \{0.22, 0.35, 0.46, 0.62, 0.79\}$. The sampling kernel is chosen as

$$g(t) = \sum_{k=-K}^{K} \frac{e^{j\omega_0 k t}}{2K+1} = \frac{\sin((K+0.5)\omega_0 t)}{\sin(\omega_0 t/2)}, -\frac{T}{2} \leq t \leq \frac{T}{2}, \qquad (14)$$

which is the sum-of-sincs (SoS) kernel in the Fourier domain [24]. This choice considers $M = K$ in Eq. (9), which gives access to $2K+1$ Fourier coefficients via time-domain measurements. Consider time-encoded measurements of the filtered signal $y_1 = (x_1 * g)$ using DIF-TEM with parameters $\alpha = 16.4, \gamma = 2$. The parameters are chosen such that they critically satisfy the sampling requirement (cf. Proposition 1). We also directly encode the FRI signal using a DIF-TEM with parameters $\alpha = 100, \gamma = 2$ such that 58 measurements are recorded in the interval $[0, 1]$. For comparison, we use the zero-order hold followed by integration method of Martinez-Nuevo *et al.* [27]. The corresponding reconstruction $\bar{x}_1(t)$ is effectively a piecewise linear signal. The approximation error between $x_1(t)$ and $\bar{x}_1(t)$ vanishes when the number of measurements increases. Fig. 3(a) shows $\mathcal{D}y_1(t)$, which is the derivative of the filtered signal, the input to the Schmitt trigger $v_1(t)$ and the output of the DIF-TEM $\{t_n\}$. Fig. 3(b) shows the FRI signal $x_1(t)$, the reconstruction obtained using Prony's method $\check{x}_1(t)$ and the zero-order-hold-based reconstruction $\bar{x}_1(t)$. The reconstruction signal-to-noise (RSNR) ratio is used as the performance measure and is defined as follows:

$$\text{RSNR}(x, \check{x}) = 10\text{dB} \cdot \log_{10} \left(\frac{\|x\|_{L^2([0,T[)}^2}{\|x - \check{x}\|_{L^2([0,T[)}^2} \right). \qquad (15)$$

We found that $\text{RSNR}(x_1, \check{x}_1) = 51$ dB and $\text{RSNR}(x_1, \bar{x}_1) = 9$ dB, which indicates high reconstruction accuracy of the proposed method. Next, consider the stream of Dirac impulses

$$x_2(t) = \sum_{m \in \mathbb{Z}} \sum_{k=0}^{4} c_k \delta(t - \tau_k - m), \qquad (16)$$

where the amplitudes are drawn from the standard normal distribution $\mathcal{N}(0, 1)$ and the shifts are selected uniformly at random over $[0, 1[$. Consider the SoS sampling kernel $g(t)$ (cf. Eq. (14)) and DIF-TEM parameters $\alpha = 270, \gamma = 24.4$. The parameters are chosen such that they critically satisfy Proposition 1. Fig. 4(b) shows the FRI signal $x_2(t)$ and the reconstruction $\check{x}_2(t)$. The reconstruction was found to be accurate up to numerical precision.

5. CONCLUSIONS

We proposed a novel differentiate-and-fire time-encoding machine (DIF-TEM) inspired by the functioning of the magnocellular pathways in the human vision system. Considering a linear time-varying bias, we showed that the sampling density can be controlled by the slope parameter. The problem of signal reconstruction from DIF-TEM measurements is essentially one of reconstructing signals from
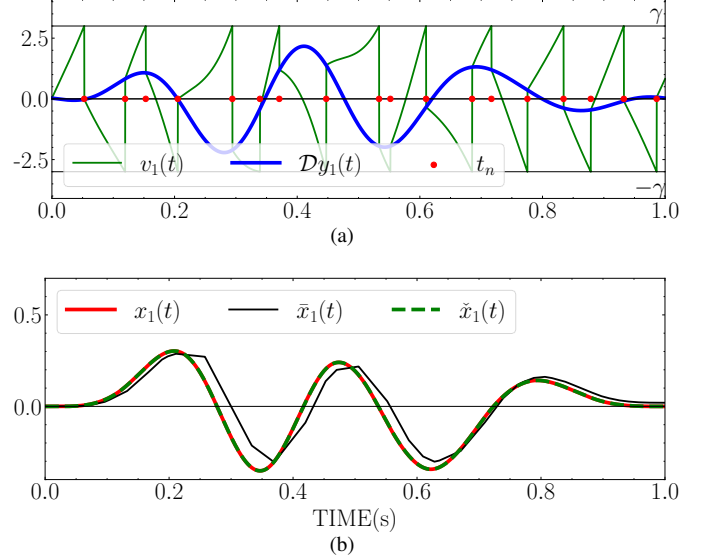

Fig. 3. Time-encoding and reconstruction using DIF-TEM: (a) shows the derivative of the filtered signal $\mathcal{D}y_1(t)$, the input to the Schmitt trigger $v_1(t)$, and the corresponding trigger times $\{t_n\}$; and (b) shows the input $x_1(t)$ and reconstructions $\check{x}_1(t)$ (proposed) and $\bar{x}_1(t)$ (from [27]).
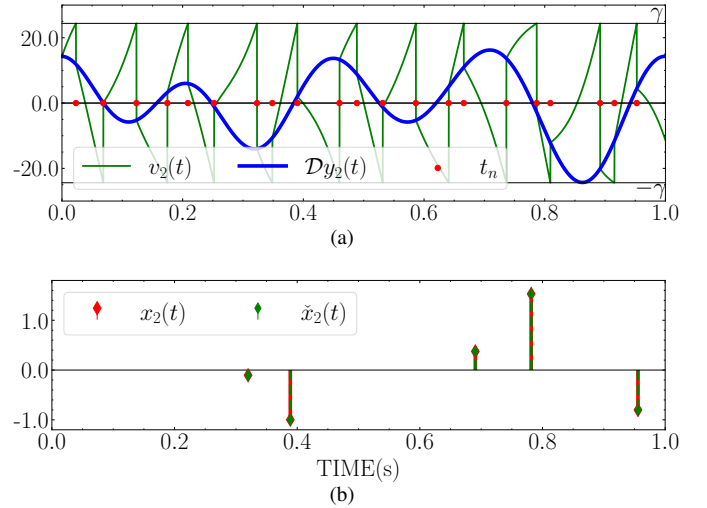

Fig. 4. Time-encoding and reconstruction using DIF-TEM: (a) shows the derivative of the filtered signal $\mathcal{D}y_2(t)$, the input to the Schmitt trigger $v_2(t)$, and the corresponding trigger times $\{t_n\}$; and (b) shows the input $x_2(t)$ and reconstructions $\check{x}_2(t)$

nonuniform samples of the derivative of the signal. We showed how the DIF-TEM can be used to encode FRI signals, and demonstrated time-encoding of the canonical periodic linear combination of time-shifted pulses. By means of Fourier-domain analysis, we showed that the FRI signal can be recovered up to a global constant offset. We provided sufficient conditions that ensure perfect reconstruction and substantiated the claims by means of simulations. Noise-robust design of the DIF-TEM and the problem of estimating the global constant offset are interesting directions for future work.

6. REFERENCES

[1] M. Unser, "Sampling-50 years after Shannon," *Proc. IEEE*, vol. 88, no. 4, pp. 569–587, 2000.

[2] C.E. Shannon, "Communication in the presence of noise," *Proceedings of the IRE*, vol. 37, no. 1, pp. 10–21, 1949.

[3] E.D. Adrian, "The Basis of Sensation: The Actions of Sense Organs," Tech. Rep., Christophers, London, 1928.

[4] A.N. Burkitt, "A review of the integrate-and-fire neuron model: I. Homogeneous synaptic input," *Biological Cybernetics*, vol. 95, no. 1, pp. 1–19, 2006.

[5] A.A Lazar, "Time encoding with an integrate-and-fire neuron with a refractory period," *Neurocomputing*, vol. 58, pp. 53–58, 2004.

[6] D. Gontier and M. Vetterli, "Sampling based on timing: Time encoding machines on shift-invariant subspaces," *Appl. Comput. Harmon. Anal.*, vol. 36, no. 1, pp. 63–78, 2014.

[7] K. Adam, A. Scholefield, and M. Vetterli, "Sampling and reconstruction of bandlimited signals with multi-channel time encoding," *IEEE Trans. Signal Process.*, vol. 68, pp. 1105–1119, 2020.

[8] T. Delbrück, B. Linares-Barranco, E. Culurciello, and C. Posch, "Activity-driven, event-based vision sensors," in *Proc. IEEE Int. Symp. Circuits Syst. (ISCAS)*, 2010, pp. 2426–2429.

[9] C. Brandli, R. Berner, M. Yang, S.C. Liu, and T. Delbruck, "A 240×180 130 dB 3 μs latency global shutter spatiotemporal vision sensor," *IEEE J. Solid-State Circuits*, vol. 49, no. 10, pp. 2333–2341, 2014.

[10] G. Gallego et al., "Event-based vision: A survey," *CoRR*, vol. abs/1904.08405, 2019.

[11] C. Scheerlinck, N. Barnes, and R. Mahony, "Continuous-time intensity estimation using event cameras," in *Asian Conf. Comput. Vis. (ACCV)*, December 2018, pp. 308–324.

[12] A.H.C van der Heijden, *Selective Attention in Vision*, Routledge, 2003.

[13] A.J. Kamath and C.S Seelamantula, "Neuromorphic sampling," in *Conf. Rec. Asilomar Conf. Signals Syst. Comput. (ACSSCS) (invited talk, no paper associated)*, 2021.

[14] M. Vetterli, P. Marziliano, and T. Blu, "Sampling signals with finite rate of innovation," *IEEE Trans. Signal Process.*, vol. 50, no. 6, pp. 1417–1428, June 2002.

[15] F. Marvasti, *Nonuniform sampling: Theory and Practice*, Springer Science & Business Media, 2012.

[16] R.J. Marks, *Introduction to Shannon Sampling and Interpolation Theory*, Springer Science & Business Media, 2012.

[17] A.J. Kamath, S. Rudresh, and C.S. Seelamantula, "Time encoding of finite-rate-of-innovation signals," `https://arxiv.org/abs/2107.03344`, 2021.

[18] C.S. Seelamantula, "A sub-Nyquist sampling method for computing the level-crossing-times of an analog signal: Theory and applications," in *Proc. IEEE Int. Conf. Signal Process., Comm. (SPCOM)*, 2010, pp. 1–5.

[19] Y.M. Lu and M.N. Do, "A theory for sampling signals from a union of subspaces," *IEEE Trans. Signal Process.*, vol. 56, no. 6, pp. 2334–2345, 2008.

[20] P. Stoica and R. Moses, *Introduction to Spectral Analysis.*, Englewood Cliffs, NJ, USA: Prentice-Hall, 2000.

[21] G.R. deProny, "Essai experimental et analytique: Sur les lois de la dilatabilité de fluides élastiques et sur celles de la force expansive de la vapeur de l'eau et de la vapeur de l'alcool, à différentes températures," *J. de l'Ecole Polytechnique*, vol. 1, no. 2, pp. 24–76, 1795.

[22] R.A. Horn and C.R. Johnson, *Matrix Analysis*, Cambridge University Press, USA, 2nd edition, 2012.

[23] S. Mulleti and C.S. Seelamantula, "Paley−Wiener characterization of kernels for finite-rate-of-innovation sampling," *IEEE Trans. Signal Process.*, vol. 65, no. 22, pp. 5860–5872, 2017.

[24] R. Tur, Y.C. Eldar, and Z. Friedman, "Innovation rate sampling of pulse streams with application to ultrasound imaging," *IEEE Trans. Signal Process.*, vol. 59, no. 4, pp. 1827–1842, Apr. 2011.

[25] P.L. Dragotti, M. Vetterli, and T. Blu, "Sampling moments and reconstructing signals of finite rate of innovation: Shannon meets Strang-Fix," *IEEE Trans. Signal Process.*, vol. 55, no. 5, pp. 1741–1757, May 2007.

[26] M. Unser, "Splines: a perfect fit for signal and image processing," *Proc. IEEE*, vol. 16, no. 6, pp. 22–38, 1999.

[27] P. Martínez-Nuevo, S. Patil, and Y. Tsividis, "Derivative level-crossing sampling," *IEEE Trans. Circuits Syst. II Express Briefs*, vol. 62, no. 1, pp. 11–15, 2015.